

MODELING OF AIRCRAFT COMPONENT PLACEMENTS WITH BIN PACKING

Josh Chang[1] & Michael Kokkolaras[2]

[1]Department of Mechanical Engineering, McGill University, Montreal, Quebec, Canada
[2]School of Mechanical and Automotive Engineering, Clemson University, Clemson, South Carolina, United States

Abstract

Taking into account component interactions is required to quantify the impact of integrating new systems into an aircraft during conceptual design. These interactions depend on the positions of aircraft components and require physics-based modeling to assess their feasibility. Moreover, their incorporation into a design optimization process necessitates a model to describe where components can be placed. A modified three-dimensional bin packing model is proposed to achieve this, as well as to permit approximation of wire weight and safety requirements.

Keywords: system placement, component placement, optimization, conceptual aircraft design

1. Introduction

The integration of new systems into existing aircraft introduces design couplings, increasing thus design complexity and requirements. According to [1], all systems must be considered during the three phases (conceptual, preliminary, and detailed) of aircraft design. While physics-based modeling is commonly used to assess aerodynamics, structures, and propulsive systems, it has not been extended often to systems feasibility [2–5]. Tfaily and Kokkolaras showed that component-level interactions can affect overall aircraft design and sizing [6]. Low-fidelity environmental, de-icing, and pneumatic considerations can impact optimized maximum takeoff weight, airframe, and wingspan when incorporated into multidisciplinary design analysis and optimization (MDAO) for conceptual design.

Sanchez et al. proposed the use of computer-aided design (CAD) to assess system feasibility [7]. Proposed requirements in the literature include thermal, maintainability, and safety models and can be assessed with component placements. Sanchez et al. demonstrated the effects of thermal considerations on a set of placements with computational fluid dynamics (CFD) [8]. A simplified methodology suitable for conceptual design methodology is tested in the aft equipment bay of an aircraft, which is adjusted in a later paper [9]. Selim et al. created a simplified simulation model to define a numerical metric to quantify maintenance considerations [10]. Zonal Safety Analysis (ZSA) and Particular Risk Analysis (PRA) models have been created in unmanned aerial vehicles and aircraft while introducing discrete and discontinuous constraints [11–13].

1.1 Component Placement

Despite the existence of physics-based models to assess component placement, the complexity of optimizing existing models has resulted in minimal background literature on aircraft component placement (ACP). Ng and Leng used genetic algorithms to propose sets of system placements for a drone quadrotor with 11 components and 45 variables [14]. These heuristics utilized an excess of 4×10^5 iterations, a quantity that is likely too high for conceptual aircraft design models that would take longer

to run. For the AGILE4.0 project, Fioriti et al. placed 17 systems within an electrical equipment bay with two blackbox models using Super Efficient Global Optimization with Mixture of Experts (SEGO-MOE) [15]. However, the intersection volume constraint was not feasible at termination and required an additional gradient-based algorithm to resolve overlapping components.

In the ACP problem, large quantities of analytical constraints enforce the separation, isolation, and non-intersection of components and are "complicated" by blackbox simulation-derived constraints. Existing ACP blackbox models, while capable of modeling complex phenomena, can prevent optimization as they take seconds to run with inferior mathematical properties [16, 17].

To address the complicating constraints, Fioriti et al. used a multi-stage optimization to decompose the problem which separated blackbox constraints in an automobile component placement problem [15]. Kim et al. utilized distributed MDAO to separate models that could be solved with more efficient gradient-based solvers from those that required blackbox solvers [18]. Approaches such as Talgorn et al. allow for the segregation of these constraints in a generalized manner without restrictions on problem structure [19].

1.2 Mixed-integer Linear Programming

To permit similar methodologies to be used on ACP, models with improved mathematical properties are needed. One such methodology to design and implement these analytical constraints are cutting and packing models [20]. A set of boxes is modeled as being placed inside a larger volume, referred to as a bin or container. These problems rely upon mixed-integer linear programming (MILP) that can be solved more efficiently and robustly than blackbox models.

While MILP models are limited in how they can describe engineering principles, they provide faster convergence and stronger mathematical properties than blackbox models. Optimization algorithms solving MILP models can provide estimates that are orders of magnitude faster than blackbox models. When given an objective to minimize or maximize, such as the weight of a design, mathematical guarantees are provided on the minimum and maximum objective that will be found. Known as primal and dual bounds, MILP can efficiently rule out designs and find globally optimal solutions [21].

To this end, it is proposed that aspects of the ACP problem can be modeled with a modified three-dimensional bin packing (3DBP) problem, as defined in Chen et al. [22]. A model formulation to satisfy engineering requirements at a low-fidelity level during conceptual design is demonstrated. The proposed model can perform a simplified ACP analysis or be incorporated with higher-fidelity physics-based models with MDAO. Finally, a case study with the placement of avionics components in a series of equipment racks is shown.

2. Methodology

In this paper, aircraft components that can be placed on the shelves of an aircraft equipment bay can be modeled as shown in Figure 1. These components, interchangeably referred to as boxes, and the shelves are modeled as axis-aligned rectangular prisms in a Cartesian coordinate system. Geometries of boxes, indexed by $i \in I$, are placed within shelves of an equipment bay, indexed by $j \in J$, of predefined locations and sizes. Locations are defined using the front-left bottom corner of boxes, x_i, y_i, z_i, and equipment bay shelves, X_j, Y_j, Z_j.

The Cartesian coordinate system in this paper uses x for the forward and aft directions, y for lateral movement, and z for up and down. The base model, made of modified 3DBP constraints, g_{bp} are defined in Section 2.1 to ensure designs are "geometrically feasible" or could fit within the equipment bay. These constraints ensure there is no overlap between a box and the equipment bay or another box. It can be used in conjunction with simulation or blackbox models to assess other engineering requirements such as thermal risk or maintainability to define potentially feasible system layouts.

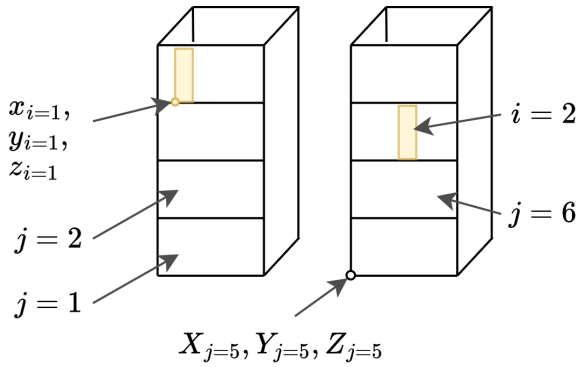


Figure 1 – Nomenclature of aircraft bin packing problem.

However, modifications to this base model can be made to assess engineering considerations and requirements at the conceptual design fidelity level. Additional constraints for modeling ZSA requirements, g_s, are described in Section 2.3. A low-fidelity wire estimate, f_w, and wire routing model, g_w, are described in Section 2.2. Problem (1) summarizes the overall problem demonstrated in this paper.

$$\begin{aligned} \min_{x_i, y_i, z_i} \quad & f_w \\ \text{s.t.} \quad & g_{bp} \leq 0, \\ & g_s \leq 0, \\ & g_w \leq 0. \end{aligned} \tag{1}$$

In this problem, minimization of wiring weight is achieved with changes to the placement of components as described by their Cartesian coordinate. These box placements must meet user-defined safety criteria and be geometrically feasible.

2.1 Packing Model

The utilized packing model is a simplification of Chen et al.; its equations for box rotation and objective are removed [22]. Table 1 defines and describes all parameters and variables for bin packing in addition to the units utilized for the paper. In this paper, parameters describe the problem, are held constant for a given optimization problem, and are denoted by capital letters. Variables are changed by an optimization algorithm and denoted by lowercase letters.

Table 1 – Parameters and Variables for Bin Packing Model

Symbols	Description	Units
	Parameters	
P_i, Q_i, R_i	Length, width, and height of boxes	in
L_j, W_j, H_j	Length, width, and height of equipment racks	in
M	Arbitrarily large value	-
	Variables	
x_i^l, y_i^l, z_i^l	Local coordinate of box in equipment rack	in
a_{ik}, b_{ik}	If box i is forward or aft of box k	-
c_{ik}, d_{ik}	If box i is left or right of box k	-
e_{ik}, f_{ik}	If box i is above or below of box k	-
s_{ij}	If box i is in equipment rack j	-

Similarly to 3DBP, the length, width, and height of components and equipment racks are defined with P_i, Q_i, R_i and L_j, W_j, H_j respectively. Length is aligned along the x direction, width with the y direction,

and height along the z direction. If box i is on equipment rack j, the indicator variable s_{ij} is equal to 1. Each box can only be in one equipment rack at any given time as enforced by Equation 2.

$$\sum_{j \in J} s_{ij} = 1 \quad \forall i \in I. \tag{2}$$

The position of the box is then described in local Cartesian coordinates (x_i^l, y_i^l, z_i^l) relative to the front-left bottom corner of the container it is in. To avoid intersection with the equipment rack, Equation 3 ensure the dimensions of the box do not exceed the equipment rack boundary it is in.

$$0 \leq x_i^l \leq L_j + (1 - s_{ij}) \cdot M - P_i, \tag{3a}$$
$$0 \leq y_i^l \leq W_j + (1 - s_{ij}) \cdot M - Q_i, \tag{3b}$$
$$0 \leq z_i^l \leq H_j + (1 - s_{ij}) \cdot M - R_i \quad \forall i \in I, j \in J. \tag{3c}$$

Box-to-box intersection is considered by identifying the relative position of every pair of boxes. Each of the indicator variables a, b, c, d, e, f describe this relative positioning along a particular Cartesian axis. For example, a considers if the maximum x-coordinate of box i is less than the minimum x-coordinate of box k. Indicator constraints are equal to 1 if a box i is to the forward, aft, left, right, below, or above of box k for a, b, c, d, e, f respectively, as illustrated in Equation 4.

$$x_i^l + P_i \leq x_k^l + (1 - a_{ik}) \cdot M, \tag{4a}$$
$$x_k^l + P_k \leq x_i^l + (1 - b_{ik}) \cdot M, \tag{4b}$$
$$y_i^l + Q_i \leq y_k^l + (1 - c_{ik}) \cdot M, \tag{4c}$$
$$y_k^l + Q_k \leq y_i^l + (1 - d_{ik}) \cdot M, \tag{4d}$$
$$z_i^l + R_i \leq z_k^l + (1 - e_{ik}) \cdot M, \tag{4e}$$
$$z_k^l + R_k \leq z_i^l + (1 - f_{ik}) \cdot M \quad \forall i, k \in I \quad \text{such that} \quad i < k. \tag{4f}$$

For every pair of boxes, they must either: 1) not be in the same equipment rack, or 2) have at least one indicator variable set to true, or equal to 1, as described in Equation 5.

$$a_{ik} + b_{ik} + c_{ik} + d_{ik} + e_{ik} + f_{ik} \geq s_{ij} + s_{kj} - 1 \quad \forall i, k \in I, j \in J \quad \text{such that} \quad i < k. \tag{5}$$

2.2 Wiring Model

To approximate the wiring weight of a particular set of system placements, two types are wires are modeled. Wires between two boxes, indexed with $i, k \in I$, involve two components with variable location in the equipment racks. Additionally, wires can be modeled between a box and a fixed point in the aircraft, such as between a box and the cockpit. This fixed point is described with Cartesian coordinates X_f, Y_f, Z_f indexed with $(i, f) \in F$ and can be outside of the defined equipment racks.

This wire weight approximation involves an estimation of wire length, as described in Section 2.2.1 , and a predefined wire thickness. This approximation defines potential wire weight increases or decreases in an aircraft design problem when placements are moved. The thickness of each wire is quantified by a line density, ρ, or the weight per unit length of each wire. If greater than zero, a wire exists and provides a lower bound on the weight of the wire. The necessary parameters for the proposed model are summarized in Table 2.

The weight of wires to fixed points, m_{if}, and between boxes, m_{ik} are summed to define the total wiring weight of the design as shown in Equation 6.

Table 2 – Parameters and Variables for Wiring Estimation

Symbols	Description	Units
	Parameters	
F	Set of box indices for fixed wires	-
X_f, Y_f, Z_f	Cartesian coordinates of fixed points	in
ρ_{if}, ρ_{ik}	Line density for a wire	lb/in
E^a	Equipment rack set in above-floor bays	-
E^u	Set of all under-floor equipment racks	-
Z_g	Height of the aircraft floor	in
	Variables	
d_{if}, d_{ik}	Distance of a wire	in
m_{if}, m_{ik}	Weight of a wire	lb
w_{ik}, w_{if}	If wire routing constraint is active	-
x_i, y_i, z_i	Global coordinate of box in design	in

$$f_w = \sum_{i,k \in I,\, i<k} m_{ik} + \sum_{(i,f) \in F} m_{if}. \tag{6}$$

In addition to user-defined parameters in Table 2, wiring weight varies on the rectilinear distance between the endpoints, as described in Section 2.2.1. Additionally, wire routing constraints, described in Section 2.2.2, define situations where a rectilinear distance between the endpoints of a wire is insufficient for wire length estimation.

2.2.1 Estimation of wire length

The length of an aircraft equipment bay is assumed to be approximately the difference between the two endpoints using the 1-norm rectilinear distance. This is calculated with the absolute differences in the box positions in a global Cartesian coordinate system x_i, y_i, z_i as shown in Equation 7. The local Cartesian coordinate is added to the front-left bottom point of the container X_j, Y_j, Z_j if $s_{ij} = 1$.

$$x_i = x_i^l + \sum_{j \in J} s_{ij} X_j \quad \forall i \in I, \tag{7a}$$

$$y_i = y_i^l + \sum_{j \in J} s_{ij} Y_j \quad \forall i \in I, \tag{7b}$$

$$z_i = z_i^l + \sum_{j \in J} s_{ij} Z_j \quad \forall i \in I. \tag{7c}$$

For two boxes, distance d_{ik} is defined with a lower-bounded absolute difference as illustrated in Equation 8. This distance calculation is only suitable when an increase in distance is of opposing monotonicity to the objective and constraints.

$$-d_{ik}^x \leq x_i - x_k + 0.5P_i - 0.5P_k \leq d_{ik}^x \quad \forall i,k \in I, \tag{8a}$$

$$-d_{ik}^y \leq y_i - y_k + 0.5Q_i - 0.5Q_k \leq d_{ik}^y \quad \forall i,k \in I, \tag{8b}$$

$$-d_{ik}^z \leq z_i - z_k + 0.5R_i - 0.5R_k \leq d_{ik}^z \quad \forall i,k \in I \quad \text{such that} \quad i < k. \tag{8c}$$

The overall distance, is then the summation of each of the Cartesian components summarized in Equation 9.

$$d_{ik} = d_{ik}^x + d_{ik}^y + d_{ik}^z \quad \forall i,k \in I \quad \text{such that} \quad i < k. \tag{9}$$

A similar calculation can be repeated for wires to fixed points, which are defined in a set that identify the box, $(i,f) \in F$, and position, X_f, Y_f, Z_f where it is wired to as shown in Equation 10.

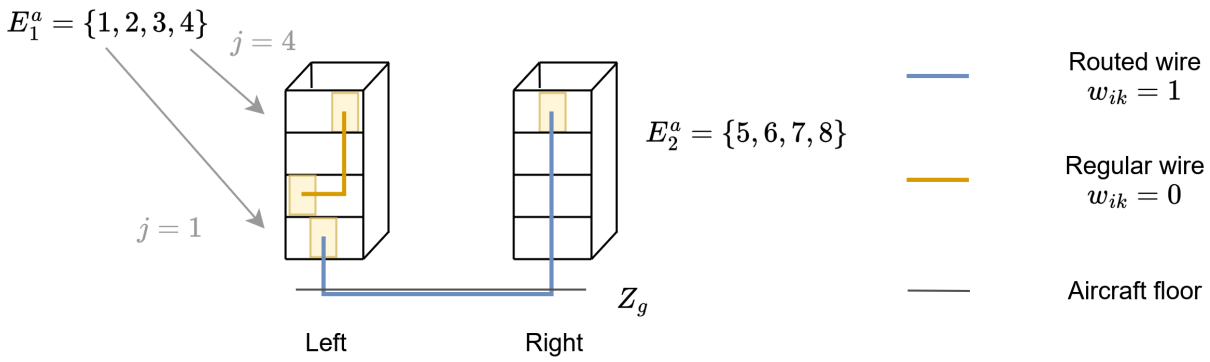


Figure 2 – Aircraft equipment bays and wire routing example.

$$-d_{if}^x \leq x_i - X_f \leq d_{if}^x \quad \forall (i,f) \in F, \tag{10a}$$
$$-d_{if}^y \leq y_i - Y_f \leq d_{if}^y \quad \forall (i,f) \in F, \tag{10b}$$
$$-d_{if}^z \leq z_i - Z_f \leq d_{if}^z \quad \forall (i,f) \in F. \tag{10c}$$

An initial wiring weight estimate is the line density of a given wire multiplied by its distance along each Cartesian axis as shown in Equation 11.

$$m_{ik}^x \geq \rho_{ik} d_{ik}^x, \quad m_{ik}^y \geq \rho_{ik} d_{ik}^y, \quad m_{ik}^z \geq \rho_{ik} d_{ik}^z \quad \forall i,k \in I \quad \text{such that} \quad i < k, \tag{11a}$$
$$m_{if}^x \geq \rho_{if} d_{if}^x, \quad m_{if}^y \geq \rho_{if} d_{if}^y, \quad m_{if}^z \geq \rho_{if} d_{if}^z \quad \forall (i,f) \in F. \tag{11b}$$

Finally, the mass of each wire is the sum of all three of its Cartesian components as defined in Equation 12

$$m_{ik} = m_{ik}^x + m_{ik}^y + m_{ik}^z \quad \forall i,k \in I \quad \text{such that} \quad i < k, \tag{12a}$$
$$m_{if} = m_{if}^x + m_{if}^y + m_{if}^z \quad \forall (i,f) \in F. \tag{12b}$$

2.2.2 Wire routing

Wire routing constraints are used to define situations in which a wire between two boxes must be elongated beyond the minimum distance. A wire between two boxes in two different above-floor equipment bays must first pass below the floor of the aircraft, Z_g, as wires cannot cross through the aircraft cabin. "Crossover" wires are modeled with additional constraints to provide additional lower bounds when the wire length cannot be adequately modeled by the distance between two boxes. To achieve this, the racks belonging to each equipment bay are defined in a set $E^a \subseteq J$ as shown in Figure 2.

All above floor equipment bays, $E^a \in A$, are summarized with a set of equipment trays E^a. When two boxes are placed in different above-floor equipment bays, Figure 3 shows that wire routing considerations will apply. It is assumed that wire routing restrictions do not apply to racks below the aircraft floor, which are stored in $E^u \subseteq J$. The indicator variable, w_{ik}, w_{if}, is equal to 1 when this routing constraint has been applied.

For a wire connecting two boxes, the routing constraint does not apply, or $w_{ik} = 0$, if both boxes are in the same equipment bay or one of the boxes is in an under-floor equipment rack. Equations 13a and 13b provide two bounds necessary to calculate w_{ik}.

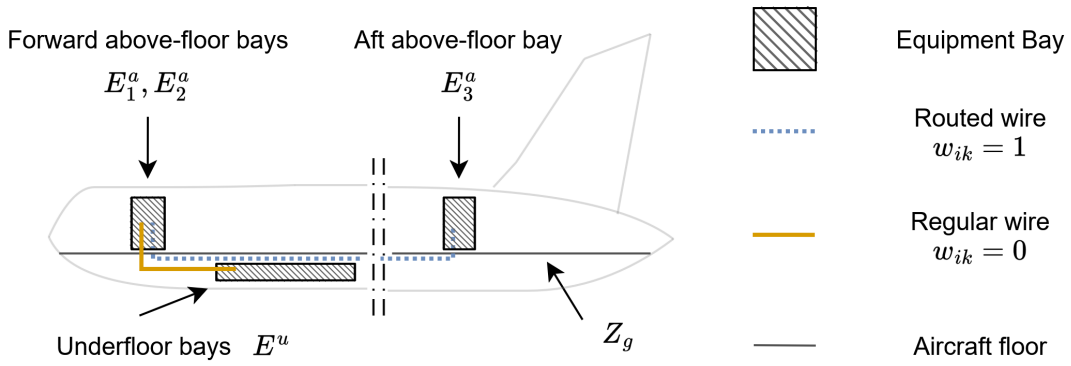


Figure 3 – Aircraft equipment bays and wire routing example.

$$\sum_{j \in E^a} s_{ij} - s_{kj} - \sum_{j \in E^u} s_{kj} \leq w_{ik} \quad \forall i,k \in I, E^a \in A \quad \text{such that} \quad i < k, \tag{13a}$$

$$\sum_{j \in E^a} s_{kj} - s_{ij} - \sum_{j \in E^u} s_{ij} \leq w_{ik} \quad \forall i,k \in I, E^a \in A \quad \text{such that} \quad i < k. \tag{13b}$$

If $w_{ik} = 1$, the length of the wire in the z-direction depends on the height of the two boxes relative to the floor, as shown in Equation 14.

$$d_{ik}^z \geq (z_k + z_i - 2Z_g) - M \cdot (1 - w_{ik}) \quad \forall i,k \in I \quad \text{such that} \quad i < k. \tag{14}$$

In contrast, for wires between a box and a fixed point, the wire routing constraint is applied if the box is in an above-floor equipment bay. Equation 15 describes this calculation.

$$\sum_{E^a \in A} \sum_{j \in E^a} s_{ij} = w_{if} \quad \forall i \in I \quad \text{such that} \quad i < k. \tag{15}$$

A minimum distance in the z direction is enforced for wires to fixed points for an active wire routing constraint as shown in Equation 16

$$d_{if}^z \geq (z_i + Z_f - 2Z_g) - M \cdot (1 - w_{if}) \quad \forall (i,f) \in F. \tag{16}$$

This constraint is only active when both $w_{if} = 1$ and the fixed point is above the aircraft floor. Otherwise, the regular Cartesian distance constraints, as described in Equation 10 will be active instead.

2.3 Safety Restrictions

In contrast to the wiring objective and constraints, which aim to reduce distance between boxes, safety restrictions enforce minimum separation between certain boxes. The list of parameters and variables used to assess safety constraints are described in Table 3.

Three approaches are shown in Figure 4 and aim to either 1) ensure sufficient spacing between boxes or 2) limit where boxes can be placed. Figure 4a describes an approach to provide separation, or a minimum distance between a group of components. Restriction in Figure 4b prevents a box from being placed in a particular equipment bay shelf. Finally, Figure 4c shows segregation which places a limit upon a group of boxes and a set of equipment bay shelves. The maximum quantity of boxes from this group which can be placed on the set of shelves is limited in number.

2.3.1 Minimum separation

The necessary space for tool and hand access during maintenance tasks can drive engineering requirements to provide empty space between components [10]. In the proposed problem, a minimum distance between components is modeled along each Cartesian axis, $\Delta_x, \Delta_y, \Delta_z$. Prior to optimization,

Table 3 – Parameters and Variables for Safety Constraints

Symbols	Description	Units
	Parameters	
$\Delta_x, \Delta_y, \Delta_z$	Min. spacing between all boxes	in
S^r	Set of box and equipment rack restrictions	-
S^h	Box set with segregation restrictions	-
T_h	Maximum number of boxes in segregation region	-
	Variables	
d_{ik}	Distance between box i and box k	-
x_i, y_i, z_i	Global coordinate of box in design	in

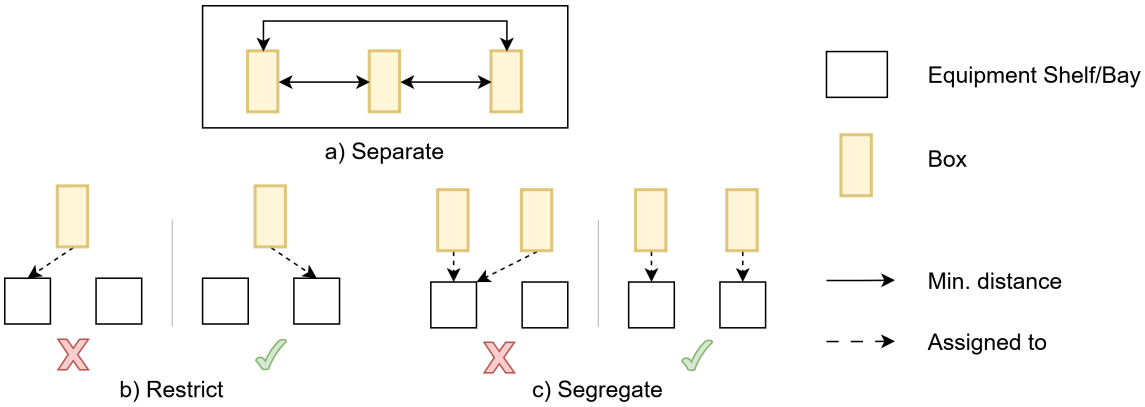


Figure 4 – Types of modeled segregation requirements.

changes to the user-provided problem parameters are made to enforce these requirements. Box sizes, equipment bay shelf sizes, and equipment bay shelf locations are modified as described in Equation 17.

$$P_i \leftarrow P_i + \Delta_x, \quad Q_i \leftarrow Q_i + \Delta_y, \quad R_i \leftarrow R_i + \Delta_z \quad \forall i \in I. \tag{17a}$$
$$L_j \leftarrow L_j + \Delta_x, \quad W_j \leftarrow W_j + \Delta_y, \quad H_j \leftarrow H_j + \Delta_z \quad \forall j \in J. \tag{17b}$$
$$X_j \leftarrow X_j - 0.5\Delta_x, \quad Y_j \leftarrow Y_j - 0.5\Delta_y, \quad Z_j \leftarrow Z_j - 0.5\Delta_z \quad \forall j \in J. \tag{17c}$$

After solving the optimization problem with these changed problem parameters, adjustments to the reported positions are required. The positions of the boxes can be adjusted by accounting for the drift in the front-left bottom corner of each box as shown in Equation 18.

$$x_i^* \leftarrow x_i^* + 0.5\Delta_x, \quad y_i^* \leftarrow y_i^* + 0.5\Delta_y, \quad z_i^* \leftarrow z_i^* + 0.5\Delta_z \quad \forall i \in I. \tag{18}$$

These adjustments do not provide extra spacing between the components and the equipment bay shelves. This can instead be achieved with a reduction in the equipment rack or bay definition for component placement.

2.3.2 Restriction

Certain components may be limited in the equipment bay shelves or locations in which they can be placed. This can be due to ZSA risk zones or placement in lower and cooler equipment racks to ensure components temperature limits are satisfied [9,13]. The list of components and corresponding equipment racks that have restrictions, as defined in S^r are set to zero as seen in Equation 19.

$$s_{ij} = 0 \quad \forall (i,j) \in S^r. \tag{19}$$

2.3.3 Segregation

Component segregation ensures that a set of boxes I_h can be isolated by limiting the total number T_h, which can be placed in a given area. This area is defined by a set of one or more predefined equipment bay shelves J_h. This can be used to provide left/right segregation for redundant components or to ensure redundant boxes are not placed on the same shelf. Equation 20 illustrates the proposed constraint to enforce this requirement.

$$\sum_{i \in I_h} \sum_{j \in J_h} s_{ij} \leq T_h \quad \forall (I_h, J_h) \in S^h. \tag{20}$$

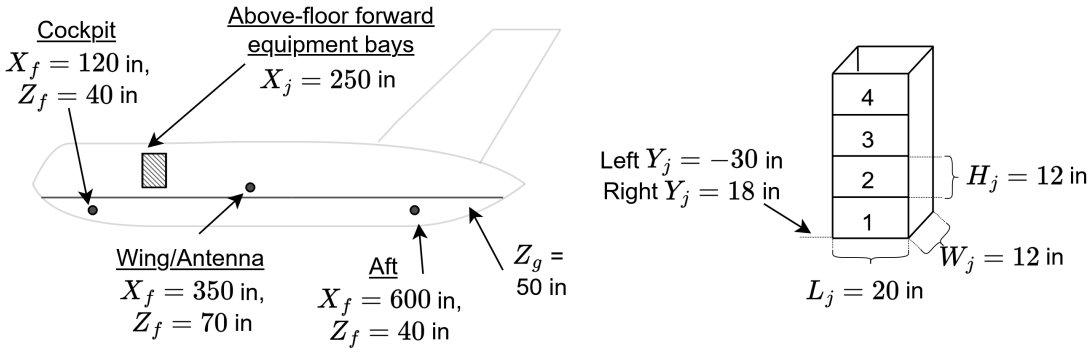
3. Results

The proposed MILP model is demonstrated with a test case of 31-line replaceable units (LRUs) to be optimized with the SCIP Optimization Suite [23]. Eight groups of three avionics or control boxes are assumed to provide redundant capability to the aircraft. Four boxes provide computational capability and additionally act as data concentrators. Finally, all avionics boxes and data concentrators are connected to one of three power distributors. All boxes are modeled with ARINC 600 geometries in modular concept units (MCU) as summarized in Table 4 [24].

Table 4 – Modeled Box Geometries and Total

Category	Description	MCU	inches	Total
a	Avionics or control	4	5.1	24
b	Data concentrators	3	3.9	4
c	Power distribution	5	7.8	3

The aircraft test case is summarized in Figure 5. Figure 5a shows the location of the two above-floor forward equipment bays (FEB) and the fixed-points that represent the tail, wing, and cockpit. Each FEB has a total of four layers, starting at $z = 70, 84, 98, 112$ in respectively as shown in Figure 5b.



a) Case study geometry and fixed points

b) Above-floor forward equipment bay geometry

Figure 5 – Test case geometry and wiring locations.

In the test case model, 1,000 wires are connected between the LRUs, power distribution, and the fixed points. The possible end-point combinations of two wires are shown in Figure 6 for box-to-box and fixed wires.

Each box receives power from one of the three power distribution boxes with a line density of $\rho = 2.5 \times 10^{-3}$ lb/in. All other wires have a line density of $\rho = 8 \times 10^{-4}$ lb/in; this includes wires between the avionics or control boxes, data computing and concentrators, and the three fixed points in the aircraft. As both FEB are above the aircraft floor, both the wiring distance constraints in Section 2.2.1 and the wire routing restrictions in Section 2.2.2 are applied.

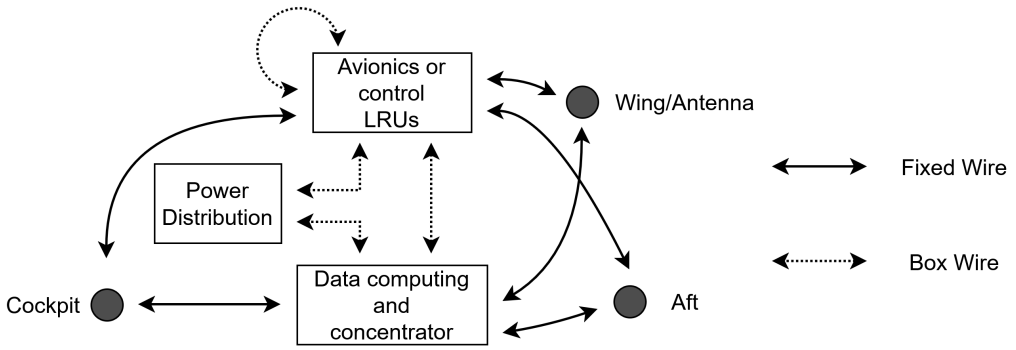


Figure 6 – Test case model wire summary.

For ZSA considerations, four requirements, as summarized in Table 5, are created. A minimum spacing of 1.5 inches between boxes is provided for tool access and maintenance tasks. Power distribution boxes are assumed to generate significant thermal loads and not be suitable for the highest shelf in both FEB. Redundancy between boxes of the same group is ensured by segregation in both the equipment bays and each individual shelf using the methodology in Section 2.3.3.

Table 5 – Modeled Box Geometries and Total

Req.	Boxes	Section	Reason
1	All	2.3.1	Boxes shall be separated by a minimum distance of 1.5 in.
2	Power	2.3.2	No power distribution box is to be placed in the highest shelf.
3	All	2.3.3	No more than 2 boxes of the same group/type per FEB.
4	All	2.3.3	No more than 1 box of the same group/type per shelf.

3.1 Optimization and Findings

The SCIP optimizer is used with the concurrent solving mode with a total of 16 threads for a total of 500 seconds of wall time. The placement of components of the design are illustrated in Figure 7. Boxes are shown as solid rectangles for avionics/control boxes (AV), cross hatched rectangles for computing and data concentrator boxes (COMP/CONC), and single hatched rectangles for power boxes (POWER DIST).

The safety requirements in Table 5 are satisfied in the proposed design from SCIP. The group number corresponding to the function of avionics and control boxes is displayed on the second row. Minimum spacing is present in the design and the group segregation per FEB and by shelf can be observed. Power distribution boxes are placed exclusively in the lower two shelves and are not on the highest shelf of either FEB.

SCIP provides the objective, or design weight, of the best design in addition to the dual objective. The best feasible design had a weight of 164.5 lb; the dual objective was 141.4 lb for a duality gap of 16.37%. It is emphasized that the dual objective does not represent the weight of the optimal design, but instead is the best possible design that can be theoretically obtained given the existing iterates. The dual objective increases with optimization iterations as we gain information through iteration.

The optimizer likely needs to reduce the quantity or weight of crossover wires due to the increased weight of routing wires below the aircraft floor. Notably, all computing and data concentrator boxes are placed in the lower two shelves on both FEB likely due to the large quantity of wires they possess. It is theorized that boxes with high line densities to other boxes and fixed points are likely to be placed upon the lower shelves. This includes the computing and data concentrator boxes in addition to the power distribution boxes.

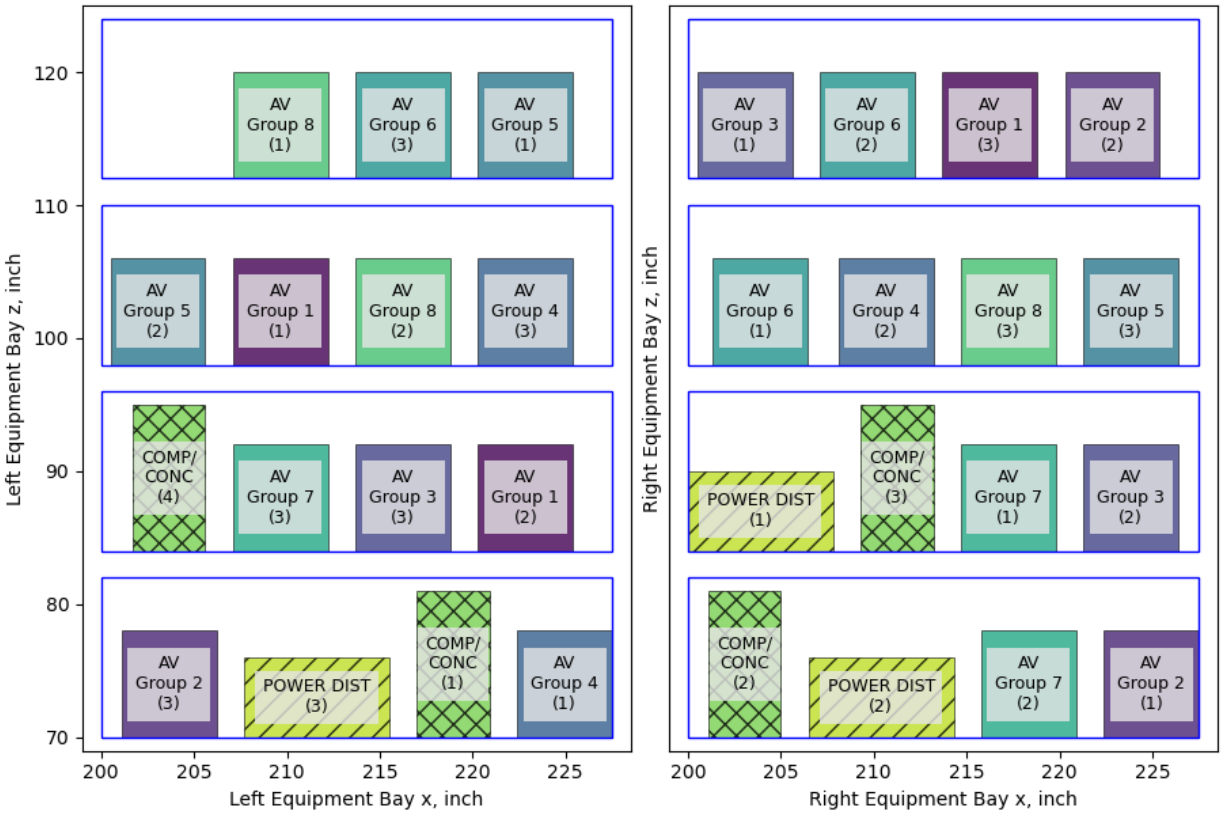


Figure 7 – Component placements of proposed model and SCIP optimizer.

4. Conclusion

The capability of using MILP models to place components in aircraft equipment bays is proposed. A series of mathematical equations modified from Chen et al. are used to define aircraft component geometries and the available space in aircraft equipment bays [22]. A list of constraints are used to define geometrically feasible designs, or when components avoid intersection with other components and the equipment bay shelves and bays.

Extensions of this baseline model are described to consider ZSA requirements and wiring weight at conceptual design fidelity levels. This demonstrates existing optimization algorithms can be used to propose component placements in an above-floor FEB test case.

To assess the capability of the proposed model to assist conceptual aircraft design, its incorporation into MDAO frameworks is proposed. Building upon past research on the importance of incorporating parametric CAD models, the creation of MILP models suitable for optimization is necessary to sufficiently explore the design space [7]. Future work to incorporate simulation based or blackbox considerations may permit higher fidelity modeling of engineering requirements to provide realistic and feasible wiring weight reductions at the conceptual design stage.

5. Contact Author

mailto: josh.chang@mail.mcgill.ca

6. Acknowledgments

This work is supported by the Natural Sciences and Engineering Research Council of Canada (NSERC) through the Postgraduate Scholarships - Doctoral (PGS D) program. Additional support is provided by NSERC, the Consortium de recherche et d'innovation en aérospatiale au Québec (CRIAQ), Bombardier, MTLS Aerostructure, and Stream Systems through a joint research project with grant number ALLRP 576486-22.

The authors would like to acknowledge Ali Tfaily, from Bombardier Aviation, for his assistance on the design of the test case. We thank Yevgen Pylayev, Alvaro Michel Tamayo, and Antoine DeBlois from Bombardier Aviation

and Susan Liscouët-Hanke from Concordia University for conversations regarding aircraft design considerations.

Cette recherche a été financée par le Conseil de recherches en sciences naturelles et en génie du Canada (CRSNG) dans le cadre du programme de Bourses d'études supérieures au niveau du doctorat (ES D). Un soutien supplémentaire est apporté par CRSNG, le Consortium de recherche et d'innovation en aérospatiale au Québec (CRIAQ), Bombardier, MTLS Aerostructure et Stream Systems dans le cadre d'un projet de recherche commun portant le numéro de subvention ALLRP 576486-22.

Les auteurs tiennent à remercier Ali Tfaily, de Bombardier Aviation, pour son aide dans la conception du scénario d'essai. Nous remercions également Yevgen Pylayev, Alvaro Michel Tamayo et Antoine DeBlois, de Bombardier Aviation, ainsi que Susan Liscouët-Hanke, de l'Université Concordia, pour leurs échanges concernant les aspects liés à la conception des avions.

7. Copyright Statement

The authors confirm that they, and/or their company or organization, hold copyright on all of the original material included in this paper. The authors also confirm that they have obtained permission, from the copyright holder of any third party material included in this paper, to publish it as part of their paper. The authors confirm that they give permission, or have obtained permission from the copyright holder of this paper, for the publication and distribution of this paper as part of the ICAS proceedings or as individual off-prints from the proceedings.

References

[1] Mavris D, DeLaurentis D, Bandte O, and Hale M. A stochastic approach to multi-disciplinary aircraft analysis and design. 1998. doi: 10.2514/6.1998-912.

[2] Risse K, Anton E, Lammering T, Franz K, and Hoernschemeyer R. An Integrated Environment for Preliminary Aircraft Design and Optimization. 2012. doi: 10.2514/6.2012-1675.

[3] Lukaczyk T. W, Wendorff A. D, Colonno M, Economon T. D, Alonso J. J, Orra T. H, and Ilario C. SUAVE: An Open-Source Environment for Multi-Fidelity Conceptual Vehicle Design. 2015. doi: 10.2514/6.2015-3087.

[4] Zhao X, Sahoo S, Kyprianidis K, Sumsurooah S, Valente G, Rashed M, Vakil G, Hill C. I, Jacob C, Gobbin A, Bardenhagen A, Prölss K, Sielemann M, Rantzer J, and Ekstedt E, A Framework for Optimization of Hybrid Aircraft2019. doi: 10.1115/gt2019-91335.

[5] Ramm J, Rahn A, Silberhorn D, Wicke K, Wende G, Papantoni V, Linke F, Kühlen M, and Dahlmann K. Assessing the Feasibility of Hydrogen-Powered Aircraft: A Comparative Economic and Environmental Analysis. *Journal of Aircraft*, Vol. 61, No. 5, pp 1337–1353, 2024. doi: 10.2514/1.C037463.

[6] Tfaily A and Kokkolaras M, *Integrating Air Systems in Aircraft Multidisciplinary Design Optimization*, AIAA AVIATION Forum, American Institute of Aeronautics and Astronautics, 2018. doi: 10.2514/6.2018-374210.2514/6.2018-3742.

[7] Sanchez F, Liscouët-Hanke S, and Tfaily A. Improving aircraft conceptual design through parametric CAD modellers – A case study for thermal analysis of aircraft systems. *Computers in Industry*, Vol. 130, pp 103467, 2021. doi: 10.1016/j.compind.2021.103467.

[8] Sanchez F and Liscouët-Hanke S. Thermal risk prediction methodology for conceptual design of aircraft equipment bays. *Aerospace Science and Technology*, Vol. 104, No. 105946, 2020. doi: 10.1016/j.ast.2020.105946.

[9] Sanchez F, Huzaifa A. M, and Liscouët-Hanke S. Ventilation considerations for an enhanced thermal risk prediction in aircraft conceptual design. *Aerospace Science and Technology*, Vol. 108, No. 106401, 2021. doi: 10.1016/j.ast.2020.106401.

[10] Sélim S, Liscouët-Hanke S, Tfaily A, Butt A, and Alphonso B. Scoring Approach to Assess Maintenance Risk for Aircraft Systems in Conceptual Design. *Journal of Aircraft*, Vol. 60, No. 5, pp 1577–1587, 2023. doi: 10.2514/1.C037142.

[11] Chiesa S, Corpino S, Fioriti M, Rougier A, and Viola N. Zonal safety analysis in aircraft conceptual design: application to SAvE aircraft. *Proceedings of the Institution of Mechanical Engineers, Part G: Journal of Aerospace Engineering*, Vol. 227, No. 4, pp 714–733, 2012. doi: 10.1177/0954410012441430.

[12] Chen Z and Fielding J. P. A zonal safety analysis methodology for preliminary aircraft systems and structural design. *The Aeronautical Journal*, Vol. 122, No. 1255, pp 1330–1351, 2018. doi: 10.1017/aer.2018.58.

[13] Bamrah P, Liscouët-Hanke S, Tfaily A, and Tamayo A. Zonal Safety and Particular Risk Analysis for Early Aircraft Design. *Journal of Aircraft*, Vol. 62, No. 2, pp 254–269, 2025. doi: 10.2514/1.C037774.

[14] Ng T. T. H and Leng G. S. B. Design of small-scale quadrotor unmanned air vehicles using genetic algorithms. *Proceedings of the Institution of Mechanical Engineers, Part G: Journal of Aerospace Engineering*, Vol. 221, No. 5, pp 893–905, 2007. doi: 10.1243/09544100jaero113.

[15] Fioriti M, Hansmann P, and Torrigiani F. Certification Driven Stream MDO Framework Descriptions And Trade Of Results. Report, 2023.

[16] Muyenzikazi N and Liscouet-Hanke S. Automation of Aircraft Maintenance Risk Assessment Using a Parametric Geometry Modeler. 2025. doi: 10.2514/6.2025-3501.

[17] Setty B. L and Liscouët-Hanke S. Automation of Wire Routing for Aircraft Conceptual Design. 2026. doi: 10.2514/6.2026-1686.

[18] Kim H. M, Kokkolaras M, Louca L. S, Delagrammatikas G. J, Michelena N. F, Filipi Z. S, Papalambros P. Y, Stein J. L, and Assanis D. N. Target cascading in vehicle redesign: a class VI truck study. *International Journal of Vehicle Design*, Vol. 29, No. 3, pp 199–225, 2002. doi: 10.1504/ijvd.2002.002010.

[19] Talgorn B, Kokkolaras M, DeBlois A, and Piperni P. Numerical investigation of non-hierarchical coordination for distributed multidisciplinary design optimization with fixed computational budget. *Structural and Multidisciplinary Optimization*, Vol. 55, No. 1, pp 205–220, 2016. doi: 10.1007/s00158-016-1489-z.

[20] Wäscher G, Haußner H, and Schumann H. An improved typology of cutting and packing problems. *European Journal of Operational Research*, Vol. 183, No. 3, pp 1109–1130, 2007. doi: 10.1016/j.ejor.2005.12.047.

[21] Martello S, Pisinger D, and Vigo D. The Three-Dimensional Bin Packing Problem. *Operations Research*, Vol. 48, No. 2, pp 256–267, 2000.

[22] Chen C. S, Lee S. M, and Shen Q. S. An analytical model for the container loading problem. *European Journal of Operational Research*, Vol. 80, No. 1, pp 68–76, 1995. doi: 10.1016/0377-2217(94)00002-t.

[23] Hojny C, Besançon M, Bestuzheva K, Borst S, Chmiela A, Dionísio J, Eifler L, Ghannam M, Gleixner A, Göß A, Hoen A, van der Hulst R, Kamp D, Koch T, Kofler K, Lentz J, Maher S. J, Mexi G, Mühmer E, Pfetsch M. E, Pokutta S, Serrano F, Shinano Y, Turner M, Vigerske S, Walter M, Weninger D, and Xu L. The SCIP Optimization Suite 10.0. Report, 2025.

[24] SAE International. 600-20 Air Transport Avionics Equipment Interfaces. Standard, 2017. doi: 10.4271/ARINC600-20.